Journal of Research in Clinical Medicine

J Res Clin Med, 2020, 8: 24
doi: 10.34172/jrcm.2020.024
https://jrcm.tbzmed.ac.ir

TUOMS PRESS

Original Article

The role of vagal ischemia on the destiny of Peyer's patches: first experimental study

Sevilay Ozmen[1], Onur Ceylan[1], Mehmet Dumlu Aydin[2], Erdem Karadeniz[3], Nazan Aydin[4], Elif Oral Ahiskalioglu[5], Tuba Demirci[6], İsmail Malkoç[7], Elif Demirci[1]

[1]Ataturk University, Medical Faculty, Department of Pathology, Erzurum, Turkey
[2]Ataturk University, Medical Faculty, Department of Neurosurgery, Erzurum, Turkey
[3]Ataturk University, Medical Faculty, Department of General Surgery, Erzurum, Turkey
[4]Uskudar University, Department of Psychology, Humanities and Social Sciences Faculty, Istanbul, Turkey
[5]Ataturk University, Medical Faculty Anesthesiology and Reanimation, Department of, Erzurum, Turkey
[6]Ataturk University, Medical Faculty, Department of Histology, Erzurum, Turkey
[7]Duzce University, Medical Faculty, Department of Anatomy, Erzurum, Turkey

Article info

Article History:
Received: 1 May 2020
Accepted: 5 June 2020
e-Published: 24 June 2020

Keywords:
- Intestinal immunodeficiency
- Peyer's patches
- Subarachnoid hemorrhage
- Vagal ischemia

Abstract

Introduction: The vagal network has a major potential role in the immune-life of Peyer's patches, but there is no satisfying information if vagal ischemia causes Peyer's patches (PP) disruption following subarachnoid hemorrhage (SAH).

Methods: Twenty-two rabbits were used as control (GI, n = 5), "sham" (GII, n = 5), and SAH (GIII, n = 12) groups in this experiment. 0.5 cc saline for GII and 0.5 cc autologous blood for GIII was injected into cisterna magna of the rabbits. Four weeks later, they were euthanized. Their brains, vagal nerves, nodose ganglia, Peyer's patches, and intestines were examined, using stereological methods. The Peyer's patches volumes (PPVs)/intestine volume per cubic millimeter was accepted as PP injury score based on a total of 10 points.

Results: The mean degenerated neuron densities of the nodose ganglia and degenerated axon densities of vagal nerves were $5 \pm 2/mm^3$ and $6 \pm 2/mm^2$ in the GI, $13 \pm 4/mm^3$ and $89 \pm 16/mm^2$ in the GII and $321 \pm 83/mm^3$ and $293 \pm 88/mm^2$ in GIII. The mean PPVs and PP score were $8 \pm 1 \times 10^6$ $\mu m^3/mm^3$ and 0-3 in the GI, $10 \pm 3 \times 10^6$ $\mu m^3/mm^3$ and 4-7 in the GII, and $21 \pm 5 \times 10^6$ $\mu m^3/mm^3$ and 8-10 in GIII. $P < 0.0001$ in PPV/PP score/degenerated axon densities of vagal nerves; $P < 0.0005$ in PPV/PP score/degenerated neuron densities of the nodose ganglia between GI/GIII; $P < 0.001$ in (PPV/PP score)/degenerated axon densities of vagal nerves; $P < 0.005$ in PPV/PP score/degenerated neuron densities of the nodose ganglia between GII/GIII; and $P > 0.05$ in GI/GII were noted.

Conclusion: Vagal ischemia/insult may be responsible for PP denervation, and injury-induced dangerous intestinal immunodeficiency following SAH.

Introduction

Peyer's patches (PP) host as a security castle for lymphoid cells or a trench for pathogens.[1] They function as intestinal microspheres.[2] PP and the vagal network containing the neuro-immunological web are essential components of intestinal immunity and are commonly located in the jejunum and ileum. PP shape the first intestinal barrier against pathogens.[3] Vagal fibers are found in PP, and adjacent villi.[4] Biological, physical, and chemical homeostasis are generally maintained by the vagal[5] and splanchnic nerves.[6] Also, Meissner's and Auerbach's networks, as well as thoracic spinal and solar ganglia, modulate all intestinal lymphoid organs.[7] The PP blood supply is maintained by the mesenteric arteries. Mesenteric artery spasm, induced by sacral parasympathetic network damage, may cause ischemic intestinal degeneration.[8] Onuf's nucleus originated sacral parasympathetic web ischemia can be responsible for Hirschsprung-like disease following spinal subarachnoid hemorrhage (SAH).[9] Sympathetic hyperactivity induced by vagal collapse may cause intestinal atrophy following SAH.[10] Because vagal nerve insufficiency causes dangerous pathologies in the intestinal system, vagal nerve stimulation may be an alternative application for neuro-inflammatory bowel disease[11] and ischemic intestinal disease. The electromagnetic field created by the vagal nerve is necessary for the regulation of intestinal microbiota.[12] We showed that vagal network ischemia might cause

***Corresponding Author:** Sevilay Ozmen MD, Ataturk University, Medical Faculty, Department of Pathology Erzurum Turkey, Phone +90 5337254072 Email: ertekozmen@gmail.com

denervation injuries characterized by PP enlargement and reactivity induced follicular hyperplasia in the early phase. In due course, however, vasospasm of the PP supplying arteries causes PP edema, swelling, hemorrhage, and necrosis.

Materials and Methods

Animal-study model

This experimentally induced SAH model was studied on 22 rabbits. After examination, the animals were randomly divided into the following three groups: the control group (GI, n = 5); the “sham” group (GII, n = 5), which received 0.5 cc of saline; and the study group (GIII, n = 12), which received autologous blood injections (0.5 cc) in tapering doses into their cisterna magna one time/three days for two weeks.

Following the head anteflexion position for to held in foramen magnum, 0.5 cc of autologous blood was injected over about one minute via 22-gauge needle after 0.5 cc cerebrospinal fluid aspiration.

Isoflurane was administered by a face mask, and 0.2 cc/kg of the anesthetic combination (ketamine HCl, 150 mg/1.5 cc; Xylazine HCl, 30 mg/1.5 cc; and distilled water, 1 cc) was subcutaneously injected.

Clinical-experimental data collection and results

Heart rate, respiration rate, and blood pressure values were recorded for ten days. The rabbits were fasted for six hours before surgical intervention and decapitated after balanced injectable anesthesia was induced. Their brains, vagal complexes, and intestines were extracted just after intracardiac formalin injection and then fixed in 10% formalin solution. The intestines were examined with anatomical microscopy. For histopathological analysis, microsections were taken from the whole brains, vagal complexes, and intestines intercrossing PP. Tissue sections (5 μm) were stained with hematoxylin-eosin (H&E), S100, GFAP, and TUNEL methods. Intestinal tissues were examined by the Cavalieri method. Vagal complexes and PP were reviewed by the stereological techniques described in our previous reports.[13, 14] To compare PP hyperplasia, Peyer’s patches volume (PPV) was calculated with geometrical formulas. For statistical analysis, the PP’s hyperplasia index (PPHi) was required. PPV/intestine volume is accepted as PPHi and shown as I. I values are classified into five groups (I 0-4). The geometrical grading compensated with the histopathological grading also has five categories.

In the control group, routine histopathological examination revealed lymphoid aggregates without dendritic networks under the surface epithelium. In the sham group, primary follicles with dendritic networks were observed under the surface epithelium by GFAP. In some subjects in the SAH group, secondary follicular structures with prominent germinal centers under the surface epithelium were detected. Enlarged, interconnected, abundant secondary follicles were detected in PP. Some follicles had dendritic cells without extensions and uncombined clusters in animals with strong vagal network ischemia. These histopathological features could be accepted as lymphoid follicular atrophy or necrosis. The histopathological scoring system was graded as $0+1+2+3+4=10$. A score <2 was considered normal, a score of 2-4 was considered hyperplasia, a score of 4-7 was considered gross PP enlargement, and a score >7 was considered intestinal invasion by PP (Table 1). Follicular hyperplasia initially increased the ratio of PP to small intestine volume and increased the PPHi. Over time, excessive PP hyperplasia brought the intestinal volume to zero, bringing the PPHi closer to infinity. A PPHi near zero indicates that the intestines have no efficacy and are becoming apoptotic. Necrosis of the lymphoid follicle volume approaching zero makes the PPHi equal to zero. A state equal to zero indicates that the PP is depleted in volume and that intestinal immunity is no longer present. These different histopathological responses within the SAH group were interpreted as different individual responses to the same stimulus.

Histopathological procedures

To detect ischemic vagal lesions, brain materials were sectioned crossing the vagal motor nucleus. Vagal nerve axons and nodose ganglia were embedded in the same paraffin block and sectioned horizontally. Their numbers were estimated using the stereological method. The ileum segments were cut into 5 μm paired sections per 20 μm every 20th and 21st sections to calculate the PPV. All sections were stained with H&E, S-100, GFAP, and TUNEL methods and examined with light microscopy. The total PP numbers of the intestines were estimated with the fractionatory method.[15]

To estimate the total PP numbers and volume values, the sections were embedded in paraffin blocks. They were stained with H&E and immunohistochemical (S-100, GFAP, and TUNEL) methods. The advantages of these methods are as follows: They allow particle numbers to

Table 1. Histopathological Scoring System of Peyer’s Patches

	Score
lymphoid aggregates without dendritic network under the surface epithelium	0
primary follicles with the dendritic network were observed under the surface epithelium	1
secondary follicular structures with prominent germinal centers under the surface epithelium	2
enlarged, interconnected, abundant secondary follicles detected in PP	3
lymphoid follicular atrophy or necrosis	4
Total Score	10

Score <2; considered as normal, score 2-4; considered as hyperplasia, score 4-7; considered as gross enlargement PP, score >7; considered as invaded intestine by PP.

be estimated easily. They are readily performed. They are intuitively simple. They are free from assumptions about particle shape, size, and orientation: and they are unaffected by overprotection and truncation.

Stereological analysis

Stereological methods provide reliable results to estimate particle number, material volume, and number. For this article, the stereological and Cavalieri methods have been explained in our previous studies.[9, 13, 16]

The total PPV was estimated by taking the sum of all PPVs. Each PP was considered an ellipsoid structure and its volume was calculated with the following formula:

$$Vpp = (4/3)\pi\left[(x+y+z)/3\right]^3$$

The x, y, and z are half of the radius values of the ellipsoid-shaped PP, which are coordinated on the x, y, and z apsis included in the analytical space. The total PPV was estimated using the following formula:

$$\sum Vpp = \sum_1^n nxVn$$

The physical dissector method was preferred to evaluate the numbers of living and degenerated follicle cells of PP, nodose ganglia, vagal axons, and neurons of the vagal motor nuclei. The used analytical and geometrical methods have been clearly explained in our previous studies.[9, 13, 15]

The data obtained were analyzed with the SPSS software package (SPSS® for Windows v. 12.0, Chicago, USA). The one-way ANOVA test was used and the differences were considered to be significant at $P < 0.05$.

Results

Clinical findings

Meningeal irritation signs, such as neck stiffness, decreased coma score, convulsion, and fever, as well as cardiorespiratory disturbances, were reported.

Anatomical and pathological findings

Blurred-hemorrhagic brain surface, cortical swelling, sulcal narrowing with adhesion, bloody basal cistern, thrombosed blood vessels, gyral bombing, and less extend tentorial herniations were observed in some cases (Figure 1/Base).

Histopathological findings

Microscopic views showed constructed vasa vasorum, deformed vagal axons, apoptotic axons, and apoptotic nodose ganglia neurons in the rabbits with SAH (Figure 1). Brain stem sections included ischemic vagal motor nuclei just behind the aqueduct. Apoptotic neurons were also seen (Figure 2). Normal PP and villi with abundant myenteric plexuses were observed in normal rabbits (Figure 3). Minimally enlarged atrophic/degenerated villi-PP with reactivated focuses, and follicular dendritic cells were seen in the sham group (Figure 4). Enlarged inflamed pathologic PP with importantly atrophic/degenerated villi representing denervated/atrophic Meissner's networks and reactivated focuses of PP with normal and deformed follicular dendritic cells were observed in the study group (Figures 5 and 6). An apoptotic neural network and stromal cells were observed in the rabbits with developed vagal ischemia (Figure 7). The PPHi calculation method

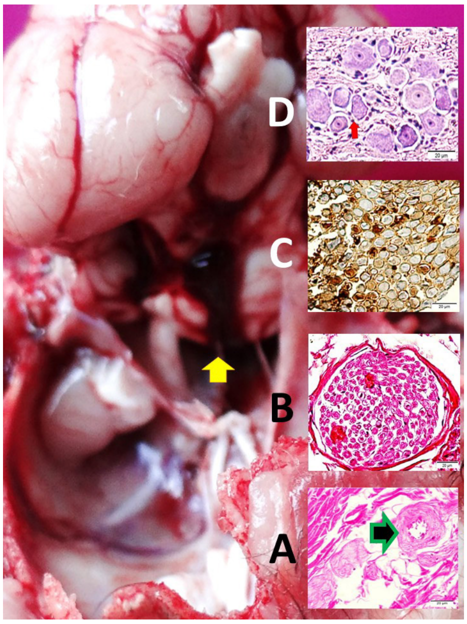

Figure 1. Macroscopic view of the basal side of the brain with SAH (Yellow arrow), constructed vasa-vasorum (arrow) and deformed axons of the vagal nerve within jugular foramen (LM, H&E, x40/A); a cross-sectional area in a normal rabbit (LM, H&E, x40/B) and apoptotic axons (LM, Tunnel, x40/C) and apoptotic nodose ganglia neurons (LM, Tunnel, x10/D) are seen with a SAH created rabbit.

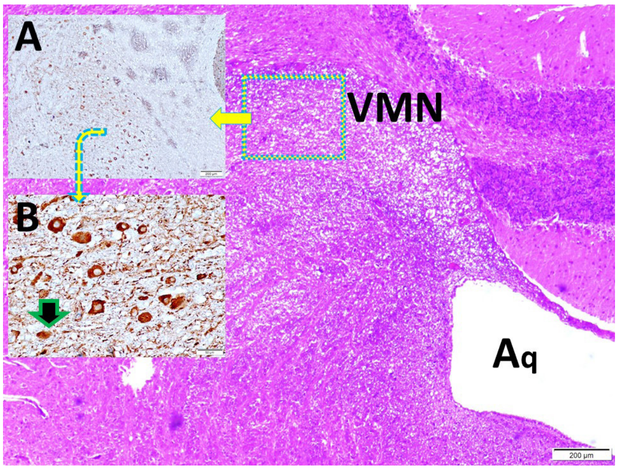

Figure 2. Histopathological view of the brain stem section including vagal motor nucleus (VMN) just behind of aqueduct (Aq) (LM, H&E, x4/Base; GFAP, x4/A); and apoptotic neurons (LM, Tunnel, x20/B) are seen in vagal ischemia developed rabbit.

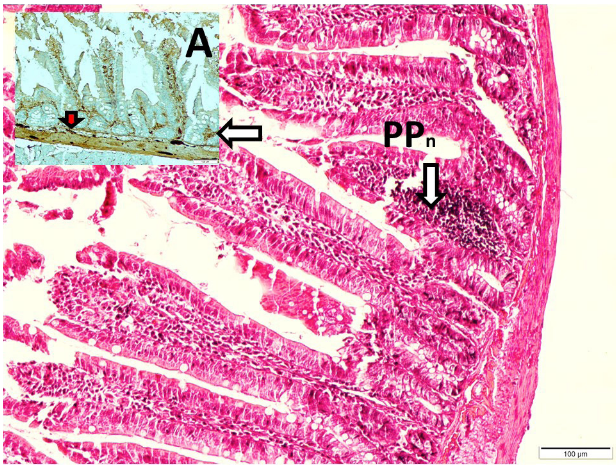

Figure 3. Histopathological view of the ileal section with normal Peyer's patches (PPn) and Willi (LM, H&E, x4/Base) and abundant myenteric plexuses (Red arrow) (LM, S-100, x10//A) are seen in a normal rabbit.

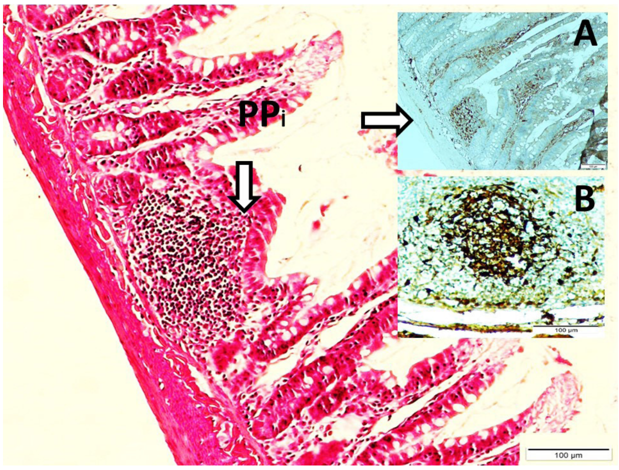

Figure 4. Histopathological view of the ileal section with a minimally enlarged pathologic Peyer's patches (PPi) with partially atrophic/degenerated Willi (LM, H&E,x4/Base; LM, S-100, x10/A); a magnified form of reactivated focus (LM, GFAP,x20/B) and follicular dendritic cells are seen in a rabbit from sham group

that was used was designed by the authors (Figure 8). More ischemic vagal injury resulted in more intestinal injury such as myenteric network deformation, intestinal glandular atrophy, and regional necrosis.

Numerical results

The rabbits with SAH showed an unconscious state at the beginning of the SAH, and two of them were dead. The mean degenerated neuron density of the nodose ganglia, and axon densities were estimated, respectively, as $5 \pm 2/mm^3$ and $6 \pm 2/mm^2$ in the control group, $13 \pm 4/mm^3$ and $89 \pm 16/mm^2$ in the sham group, and $321 \pm 83/mm^3$ and $293 \pm 88/mm^2$ in the study group. The mean PPV and histopathological scores were $8 \pm 1\times10^6$ µm^3/mm^3 and 0-3 in the control group, $10 \pm 3\times10^6$ µm^3/mm^3 and 4-7 in the sham group, and $21 \pm 5\times10^6$ µm^3/mm^3 and 8-10 in the study group. Results and p values are summarized in Table 2.

Discussion

The immunomodulatory role of vagus on PP is the critical component of intestinal immunity commonly located in the jejunum and ileum. Vagal fibers are found in PP, and adjacent villi.[4] PP form the first intestinal barrier against pathogens.[3] Physical and chemical homeostasis of the alimentary tract is sensed by the nodose ganglia and regulated by parasympathetic vagal fibers.[5] The vagal and splanchnic nerves convey information to the

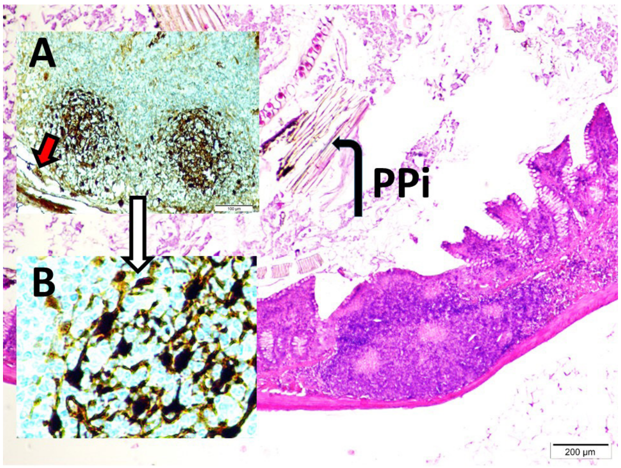

Figure 5. Histopathological view of the ileal section with an enlarged, inflamed pathologic Peyer's patches (PPi) with importantly atrophic/degenerated Willi (LM, H&E,x4/Base); representation of denervated/atrophic Meissner network (red arrow) and PP magnified form of reactivated focus with follicular dendritic cells (LM, H&E,x20) are seen in a study rabbit.

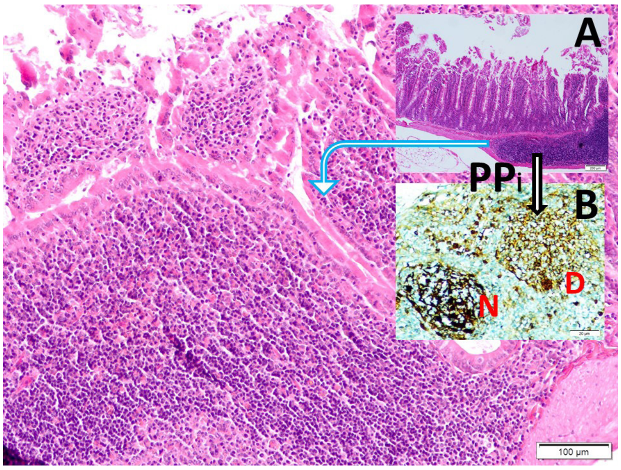

Figure 6. Histopathological view of the ileal section with an enlarged, inflamed pathologic Peyer's patches (PPi) with importantly atrophic/degenerated Willi (LM, H&E, x4/A); representation of denervated/atrophic Meissner network and PP magnified form of the reactivated focus of PP (LM, H&E, x10/Base), normal (N) and deformed (D) follicular dendritic cells (LM, GFAP, x40/B).

Table 2. Numerical results of the study

	Group I n=5)	Group II (n=5)	Group III (n=12)
Degenerated neuron density of nodose ganglia (mm^3)	5±2	13±4	321±83[a]
Degenerated axon densities (mm^3)	6±2	89±16[c]	293±88[a]
Mean volumes of Peyer's patches ($x10^6$ $\mu m^3/mm^3$)	8±1	10±3[c]	21±5[a]
Histopathological score	0-3	4-7[b]	8-10[a]

The values are given as mean ± standard deviation or median (minimum-maximum), Group I: Control Group, group II: SHAM group, group III: study group.
[a] $P < 0.0001$ Group III vs. I and II one-way ANOVA test.
[b] $P < 0.0001$ Group I vs. II one-way ANOVA test.
[c] $P < 0.005$ Group I vs. II one-way ANOVA test.

central nervous system from mechanosensory in the intestinal tract regarding the feeding of nutrients and specific endocrine-motor patterns.[6] PP can be considered intestinal microspleens.[2] PP cells modulate antibiotic-bacteria interactions.[17] Each PP has several elongated dome regions flanked by intestinal villi formed from lymphoid follicles covered with enterocytes. The interfollicular zone has high endothelial venules.[18] Phagocytes include dendritic cells, which play a significant role in mucosal homeostasis.[19] Dendritic cells are sensitive to the intestinal microenvironment and are at the front line in bacterial invasion.[20] Dendritic cells have an essential role in the first adaptive immune responses.[21] Mucosal layers of PP regulate microbiota colonization.[22] PP have selective sensitivity to digested materials.[23] Nonbiological particles undergo phagocytosis by PP cells.[24] PP synthesize most of the immunoglobulins, especially IgA.[25] Immunoglobulin synthesis primarily occurs in intestinal PP.[26]

There is mounting evidence for interactions between the PP and the vagal system. Lymphoid tissues are well supplied by somatic and autonomous nerves.[27] Oral microbiota has great importance and is regulated by the olfactory, trigeminal, and lower cranial nerves.[28] All intestinal lymphoid organs are innervated by the myenteric and solar plexuses as well as the thoracic spinal ganglia[7] because immune modulation of the enteric nervous system is required for a dense neural network. To demonstrate the enteric nervous system and PP, specific markers, such as the S-100 protein, GFAP protein, and TUNEL methods, were used. This has been mentioned by Krammer et al in their research.[29]

Dangerous histomorphological changes occur in denervated PP,[30] especially with vagal ischemia, because vagal network ischemia results in intestinal atrophy.[10] Sacral parasympathetic network ischemia causes mesenteric artery spasm related intestinal degeneration.[8] Onuf's nucleus originated from sacral parasympathetic network ischemia, can be responsible for Hirschsprung-like disease following spinal SAH.[9] Olfactory bulb lesions

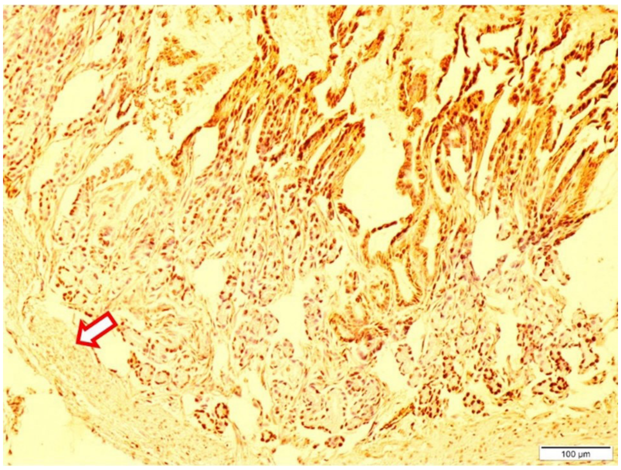

Figure 7. Histopathological view of the ileal section with apoptotic neural network and stromal cells (arrow, L&M, Tunnel, x10) in vagal ischemia developed rabbit.

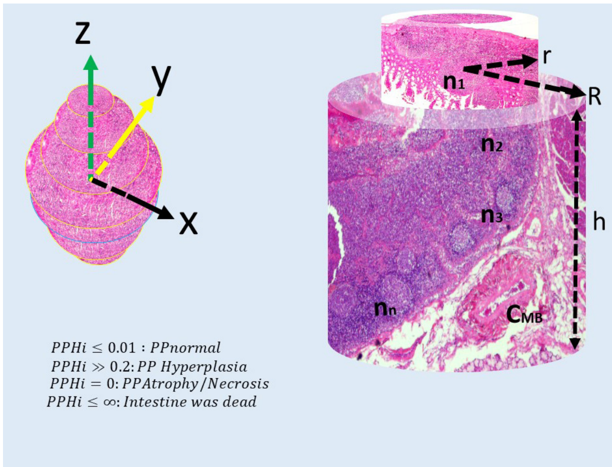

Figure 8. Peyer's patches hyperplasia index (PPHi) calculation method designed by ourselves shown as an equation $PPHi = \sum_{n=0}^{n} PP \Big/ \sum_{n=0}^{n} Vi$. Each PP is like a cylinder or sypher, and their volumes may be estimated as the following common formula: $Vpp = (4/3)\pi\left[(x+y+z)/3\right]^3$; total PP volumes were estimated as a formula: $\sum Vpp = \sum_1^n nxVn$; a cylindroid segment volume estimated as a formula $Vsi = \pi h\left(R^2 - h^2\right)$. Because PP become enlarged owing to various immunological phenomena following vagal ischemia, PP volume values will increase, and also PPHi values will be increased. Consequently, the value of the equation will be greater than zero. According to our standardization the equation should be under 0.01. If the equation is over 0.2, there is an enormous PP hyperplasia; it is equal to zero, necrosis will be started. If it approaches infinity owing to extremely PP hyperplasia, the intestine is dead. Constructed mesenteric arteries aggravate PP and intestinal necrosis.

could rely on denervation injuries of PP affected by vagal software.[13] Gut microbiota change in a dangerous manner following PP-vagal network lesions.[31] PP is the most affected part of the intestine following radiotherapy,[32] probably due to an increased intestinal electromagnetic field with the summation of magnetic fields. This theory of Wang, who justified Nikola Tesla's theory, supports our theory.

Vagal nerve stimulation may be an alternative application for immune suppression in neuroinflammatory bowel disease, a condition in which PP are the essential mediators.[11] A century ago, the great genius Nicola Tesla declared that the value of electromagnetic fields is the most crucial factor for all living things. Based on his theorem, the electromagnetic field created by the vagal nerve is an indispensable necessity for the presence of intestinal microbiota.

PP regulate the energy production, proliferation, effector functions, and metabolism of immune cells in response to the immunologic stimulus.[33] Intestinal ischemia is a necessary pathophysiological process for PP dysfunction.[34] Maternal colostrum, and milk immunoglobulins are essential for the development of strong immunity in jejunal and ileal PP.[35] Also, Liu et al. declared that ischemic stroke damages the intestinal epithelium as well as immunity.[36] Invasion by parasites, bacteria, or dangerous particles is frequently seen following ischemic intestinal disease.[37] Vagal nerve-breast network is essential for lactation, breastfeeding and the development of baby immunity.[38]

Limitations

Better results could be obtained by conducting bacteriologic, electrophysiologic, radiologic, and biochemical examinations.

Conclusion

The PP-vagal network is an excellent barrier against internal and external hazardous agents with its anti-infective, anti-tumoral, and anti-poisoning effects through its neuro-immunomodulatory functions. Although the mentioned functions of the vagal network are well known, there is no satisfying information as to whether or not vagal ischemia results in intestinal immune system hardware/software disruptions following SAH. This article demonstrates that SAH-induced vagal ischemia may be responsible for intestinal immunodeficiency by way of PP denervation injury.

Future insight

Vagal nerve stimulation or intestinal transplantation would be used for intestinal immune deficiency situations in the future.

Conflict of Interest

Authors declare no conflict of interest in this study.

Ethical Approval

Ethical approval was obtained from the ethical committee of Ataturk University Faculty of Medicine (19.09.2017/1700254064).

Authors' contributions

NA, EK, and MDA carried out the design, coordinated the study, and participated in the experiments. EOA participated in anesthesia and follow-ups. SO, OC, ED, TD participated in the examination of histopathological data. MDA. aided in statistical analysis and manuscript preparation. IM and MDA assisted in data gathering and participated in manuscript editing.

Acknowledgments

Many thanks to the pathology laboratory team.

References

1. Hashiguchi M, Kashiwakura Y, Kojima H, Kobayashi A, Kanno Y, Kobata T. Peyer's patch innate lymphoid cells regulate commensal bacteria expansion. Immunol Lett. 2015;165:1-9. doi: 10.1016/j.imlet.2015.03.002.
2. Koike R, Nishimura T, Yasumizu R, Tanaka H, Hataba Y, Hataba Y, et al. The splenic marginal zone is absent in alymphoplastic aly mutant mice. Eur J Immunol. 1996;26:669-75. doi: 10.1002/eji.1830260324.
3. Wagner C, Bonnardel J, Da Silva C, Martens L, Gorvel JP, Lelouard H. Some news from the unknown soldier, the Peyer's patch macrophage. Cell Immunol. 2018;330:159-67. doi: 10.1016/j.cellimm.2018.01.012.
4. Vulchanova L, Casey MA, Crabb GW, Kennedy WR, Brown DR. Anatomical evidence for enteric neuroimmune interactions in Peyer's patches. J Neuroimmunol. 2007;185:64-74. doi: 10.1016/j.jneuroim.2007.01.014.
5. Li BY, Schild JH. Patch clamp electrophysiology in nodose ganglia of adult rat. J Neurosci Methods. 2002;115:157-67.
6. Berthoud HR, Lynn PA, Blackshaw LA. Vagal and spinal mechanosensors in the rat stomach and colon have multiple receptive fields. Am J Physiol Regul Integr Comp Physiol. 2001;280:R1371-81. doi: 10.1152/ajpregu.2001.280.5.R1371.
7. Narita M, Kimura K, Tanimura N, Arai S, Uchimura A. Immunohistochemical demonstration of spread of Aujeszky's disease virus to the porcine central nervous system after intestinal inoculation. J Comp Pathol. 1998;118:329-36.
8. Karadeniz E, Caglar O, Firinci B, Ahiskalioglu A, Aydin MD, Kocak MN, et al. Predeterminative role of Onuf's nucleus ischemia on mesenteric artery vasospasm in spinal subarachnoid hemorrhage: a preliminary experimental study. Asian J Surg 2019;42:797-804. doi: 10.1016/j.asjsur.2018.12.004.
9. Caglar O, Firinci B, Dumlu Aydin M, Karadeniz E, Ahiskalioglu A, Sipal SA, et al. Disruption of the network between Onuf's nucleus and myenteric ganglia, and developing Hirschsprung-like disease following spinal subarachnoid haemorrhage: an experimental study. Int J Neurosci. 2019;129(11):1076-1084. doi: 10.1080/00207454.2019.1634069.
10. Cakir M, Ahiskalioglu A, Karadeniz E, Aydin MD, Malcok UA, Soyalp C, et al. A new described mechanisms of intestinal glandular atrophy induced by vagal nerve/ Auerbach network degeneration following subarachnoid hemorrhage:The first experimental study. J Clin Neurosci. 2019;59:305-9. doi: 10.1016/j.jocn.2018.10.009.
11. Willemze RA, Brinkman DJ, Welting O, Van Hamersveld

HP, Verseijden C, Luyer MD, et al. Acetylcholine-producing T-cells augment innate immune driven colitis but are redundant in T-cell driven colitis. Am J Physiol Gastrointest Liver Physiol. 2019;317(5):G557-G568. doi: 10.1152/ajpgi.00067.2019.
12. Babic RR, Stankovic Babic G, Babic SR, Babic NR. 120 years since the discovery of x-rays. Med Pregl. 2016;69:323-30.
13. Firinci B, Caglar O, Karadeniz E, Ahiskalioglu A, Demirci T, Aydin MD. Mysterious effects of olfactory pathway lesions on intestinal immunodeficiency targeting Peyer's patches: The first experimental study. Med Hypotheses. 2019;125:31-6. doi: 10.1016/j.mehy.2019.02.032.
14. Aydin MD, Kanat A, Yilmaz A, Cakir M, Emet M, Cakir Z, et al. The role of ischemic neurodegeneration of the nodose ganglia on cardiac arrest after subarachnoid hemorrhage: an experimental study. Exp Neurol. 2011;230:90-5. doi: 10.1016/j.expneurol.2010.09.018.
15. Aydin MD, Kanat A, Turkmenoglu ON, Yolas C, Gundogdu C, Aydin N. Changes in number of water-filled vesicles of choroid plexus in early and late phase of experimental rabbit subarachnoid hemorrhage model:the role of petrous ganglion of glossopharyngeal nerve. Acta Neurochir (Wien). 2014;156:1311-7. doi: 10.1007/s00701-014-2088-7.
16. Kotan D, Aydin MD, Gundogdu C, Aygul R, Aydin N, Ulvi H. Parallel development of choroid plexus degeneration and meningeal inflammation in subarachnoid hemorrhage - experimental study. Adv Clin Exp Med. 2014;23:699-704.
17. Kim SH, Jeung W, Choi ID, Jeong JW, Lee DE, Huh CS, et al. Lactic acid bacteria improves Peyer's patch cell-mediated immunoglobulin A and tight-junction expression in a destructed gut microbial environment. J Microbiol Biotechnol 2016;26:1035-45. doi: 10.4014/jmb.1512.12002.
18. Zidan M, Pabst R. Unique microanatomy of ileal peyer's patches of the one humped camel (*Camelus dromedarius*) is not age-dependent. Anat Rec (Hoboken) 2008;291:1023-8. doi: 10.1002/ar.20697
19. Morikawa M, Tsujibe S, Kiyoshima-Shibata J, Watanabe Y, Kato-Nagaoka N, Shida K, et al. Microbiota of the small intestine is selectively engulfed by phagocytes of the lamina propria and Peyer's patches. PLoS One. 2016;11:e0163607. doi: 10.1371/journal.pone.0163607.
20. Schiavi E, Smolinska S, O'Mahony L. Intestinal dendritic cells. Curr Opin Gastroenterol. 2015;31:98-103. doi: 10.1097/mog.0000000000000155.
21. Bekiaris V, Persson EK, Agace WW. Intestinal dendritic cells in the regulation of mucosal immunity. Immunol Rev. 2014;260:86-101. doi: 10.1111/imr.12194.
22. Elderman M, Sovran B, Hugenholtz F, Graversen K, Huijskes M, Houtsma E, et al. The effect of age on the intestinal mucus thickness, microbiota composition and immunity in relation to sex in mice. PLoS One. 2017;12:e0184274. doi: 10.1371/journal.pone.0184274.
23. Huang CH, Wang CC, Lin YC, Hori M, Jan TR. Oral administration with diosgenin enhances the induction of intestinal T helper 1-like regulatory T cells in a murine model of food allergy. Int Immunopharmacol. 2017;42:59-66. doi: 10.1016/j.intimp.2016.11.021.
24. Becker HM, Bertschinger MM, Rogler G. Microparticles and their impact on intestinal immunity. Dig Dis. 2012;30 Suppl 3:47-54. doi: 10.1159/000342602.
25. Butler JE, Santiago-Mateo K, Wertz N, Sun X, Sinkora M, Francis DL. Antibody repertoire development in fetal and neonatal piglets. XXIV. Hypothesis: The ileal Peyer patches (IPP) are the major source of primary, undiversified IgA antibodies in newborn piglets. Dev Comp Immunol. 2016;65:340-51. doi: 10.1016/j.dci.2016.07.020.
26. Reboldi A, Arnon TI, Rodda LB, Atakilit A, Sheppard D, Cyster JG. IgA production requires B cell interaction with subepithelial dendritic cells in Peyer's patches. Science. 2016;352:aaf4822. doi: 10.1126/science.aaf4822.
27. Stead RH. Innervation of mucosal immune cells in the gastrointestinal tract. Reg Immunol. 1992;4:91-9.
28. Garcia-Pena C, Alvarez-Cisneros T, Quiroz-Baez R, Friedland RP. Microbiota and Aging. A Review and Commentary. Arch Med Res. 2017;48:681-9. doi: 10.1016/j.arcmed.2017.11.005.
29. Krammer HJ, Kuhnel W. Topography of the enteric nervous system in Peyer's patches of the porcine small intestine. Cell Tissue Res. 1993;272:267-72. doi: 10.1007/bf00302732.
30. Heidegger S, Anz D, Stephan N, Bohn B, Herbst T, Fendler WP, et al. Virus-associated activation of innate immunity induces rapid disruption of Peyer's patches in mice. Blood. 2013;122:2591-9. doi: 10.1182/blood-2013-01-479311.
31. Ogita T, Bergamo P, Maurano F, D'Arienzo R, Mazzarella G, Bozzella G, et al. Modulatory activity of *Lactobacillus rhamnosus* OLL2838 in a mouse model of intestinal immunopathology. Immunobiology. 2015;220:701-10. doi: 10.1016/j.imbio.2015.01.004.
32. Wang H, Sun RT, Li Y, Yang YF, Xiao FJ, Zhang YK, et al. HGF gene modification in mesenchymal stem cells reduces radiation-induced intestinal injury by modulating immunity. PLoS One. 2015;10:e0124420. doi: 10.1371/journal.pone.0124420.
33. Kunisawa J. Metabolic changes during B cell differentiation for the production of intestinal IgA antibody. Cell Mol Life Sci. 2017;74:1503-9. doi: 10.1007/s00018-016-2414-8.
34. Liu L, Tan Q, Hu B, Wu H, Wang C, Liu R, et al. Somatostatin improved B cells mature in macaques during intestinal ischemia-reperfusion. PLoS One. 2015;10:e0133692. doi: 10.1371/journal.pone.0133692.
35. Le Bourgot C, Ferret-Bernard S, Le Normand L, Savary G, Menendez-Aparicio E, Blat S, et al. Maternal short-chain fructooligosaccharide supplementation influences intestinal immune system maturation in piglets. PLoS One. 2014;9:e107508. doi: 10.1371/journal.pone.0107508.
36. Liu Y, Luo S, Kou L, Tang C, Huang R, Pei Z, et al. Ischemic stroke damages the intestinal mucosa and induces alteration of the intestinal lymphocytes and CCL19 mRNA in rats. Neurosci Lett. 2017;658:165-70. doi: 10.1016/j.neulet.2017.08.061.
37. Vazeille E, Chassaing B, Buisson A, Dubois A, de Vallee A, Billard E, et al. GipA factor supports colonization of Peyer's patches by Crohn's disease-associated *Escherichia coli*. Inflamm Bowel Dis. 2016;22:68-81. doi: 10.1097/mib.0000000000000609.
38. Karadeniz E, Kocak MN, Ahiskalioglu A, Nalci KA, Ozmen S, Akcay MN, et al. Exploring of the unpredicted effects of olfactory network injuries on mammary gland degeneration:a preliminary experimental study. J Invest Surg. 2019;32:624-31. doi: 10.1080/08941939.2018.1446107.